Measurements of the branching fractions of the *P*-wave charmonium spin-singlet state $h_c(^1P_1) \to h^+h^-\pi^0/\eta$

M. Ablikim *et al.*[*]

(BESIII Collaboration)

Based on $(2712.4 \pm 14.3) \times 10^6$ $\psi(3686)$ events, we investigate four hadronic decay modes of the *P*-wave charmonium spin-singlet state $h_c(^1P_1) \to h^+h^-\pi^0/\eta$ ($h = \pi$ or K) via the process $\psi(3686) \to \pi^0 h_c$ at BESIII. The $h_c \to \pi^+\pi^-\pi^0$ decay is observed with a significance of 9.6σ after taking into account systematic uncertainties. Evidences for $h_c \to K^+K^-\pi^0$ and $h_c \to K^+K^-\eta$ are found with significances of 3.5σ and 3.3σ, respectively, after considering the systematic uncertainties. The branching fractions of these decays are measured to be $\mathcal{B}(h_c \to \pi^+\pi^-\pi^0) = (1.36 \pm 0.16 \pm 0.14) \times 10^{-3}$, $\mathcal{B}(h_c \to K^+K^-\pi^0) = (3.26 \pm 0.84 \pm 0.36) \times 10^{-4}$, and $\mathcal{B}(h_c \to K^+K^-\eta) = (3.13 \pm 1.08 \pm 0.38) \times 10^{-4}$, where the first uncertainties are statistical and the second are systematic. No significant signal of $h_c \to \pi^+\pi^-\eta$ is found, and the upper limit of its decay branching fraction is determined to be $\mathcal{B}(h_c \to \pi^+\pi^-\eta) < 4.0 \times 10^{-4}$ at the 90% confidence level.

I. INTRODUCTION

The study of charmonium states plays a central role in our understanding of quantum chromodynamics (QCD). Over the past years, the spin-singlet charmonium state $h_c(^1P_1)$ has been extensively studied, yet many of its decay modes are still unknown. The first observation of h_c was reported in 2005 by the CLEO experiment [1,2]. After that, the radiative decay $h_c \to \gamma\eta_c$ was confirmed by the Fermilab E835 [3], CLEO [4], and BESIII [5] collaborations with an average branching fraction of $(60 \pm 4)\%$ [6]. Recently, the BESIII collaboration reported the observation of several decay modes of $h_c \to$ *light hadrons*, including $h_c \to p\bar{p}\pi^+\pi^-$ [7], $h_c \to 2(\pi^+\pi^-)\pi^0$ [7], $h_c \to K^+K^-\pi^+\pi^-\pi^0$ [8], and $h_c \to 3(\pi^+\pi^-)\pi^0$ [9]. The branching fractions are of the order of 10^{-3}, and until now, the sum of the measured branching for h_c decaying to light hadrons is only 3%–4% [6]. From perturbative QCD (pQCD), the $\mathcal{B}(h_c \to$ light hadrons) is predicted to be about 48% [10], while a value of 8% is obtained from nonrelativistic QCD (NRQCD) [10]. This discrepancy between different theoretical models, as well between theory and the experimental measurements, motivates us to search for additional decay modes of the h_c and to improve the measurement precision of the known h_c decays with a larger $\psi(3686)$ data sample.

Although h_c mesons cannot be produced directly in e^+e^- collisions at BESIII, the large $\psi(3686)$ sample with $(2712.4 \pm 14.3) \times 10^6$ $\psi(3686)$ events [11] provides an opportunity to study h_c decays via the hadronic transition $\psi(3686) \to \pi^0 h_c$. In this paper, the four exclusive hadronic decays $h_c \to \pi^+\pi^-\pi^0$, $h_c \to K^+K^-\pi^0$, $h_c \to K^+K^-\eta$, and $h_c \to \pi^+\pi^-\eta$, denoted as modes I, II, III, and IV, respectively, are investigated.

II. BESIII DETECTOR AND MONTE CARLO SIMULATIONS

The BESIII detector [12] records symmetric e^+e^- collisions provided by the BEPCII storage ring [13] in the center-of-mass energy range from 2.0 to 4.95 GeV, with a peak luminosity of 1.1×10^{33} cm^{-2} s^{-1} achieved at $\sqrt{s} = 3.773$ GeV. BESIII has collected large data samples in this energy region [14–16]. The cylindrical core of the BESIII detector covers 93% of the full solid angle and consists of a helium-based multilayer drift chamber (MDC), a plastic scintillator time-of-flight system (TOF), and a CsI(Tl) electromagnetic calorimeter (EMC), which are all enclosed in a superconducting solenoidal magnet providing a 1.0 T magnetic field. The solenoid is supported by an octagonal flux-return yoke with resistive plate counter muon identification modules (MUC) interleaved with steel. The charged-particle momentum resolution at 1 GeV/c is 0.5%, and the specific energy loss (dE/dx) resolution is 6% for electrons from Bhabha scattering. The EMC measures photon energies with a resolution

---

[*]Full author list given at the end of the article.

of 2.5% (5%) at 1 GeV in the barrel (end cap) region. The time resolution in the TOF barrel region is 68 ps, while that in the end cap region was 110 ps. The end cap TOF system was upgraded in 2015 using a multigap resistive plate chamber technology, providing a time resolution of 60 ps, which benefits 83% of the data used in this analysis [17–19].

Simulated data samples produced with a GEANT4-based [20] Monte Carlo (MC) package, which includes the geometric description of the BESIII detector and the detector response, are used to determine detection efficiencies and to estimate backgrounds. The simulation models the beam energy spread and initial-state radiation (ISR) in the e^+e^- annihilations with the generator KKMC [21,22]. The inclusive MC sample includes the production of the $\psi(3686)$ resonance, the initial-state radiation production of the J/ψ, and the continuum processes incorporated in KKMC [21,22]. All particle decays are modeled with EVTGEN [23,24] using branching fractions either taken from the Particle Data Group (PDG) [6], when available, or otherwise estimated with LUNDCHARM [25,26]. Final-state radiation from charged final-state particles is included using the PHOTOS package [27]. The exclusive signal MC samples are generated by the phase space model with all the branching fractions of the intermediate states set to be 100%, and each sample contains one hundred thousand events.

III. EVENT SELECTION AND DATA ANALYSIS

Charged tracks detected in the MDC are required to be within a polar angle (θ) range of $|\cos\theta| < 0.93$, where θ is defined with respect to the z axis, which is the symmetry axis of the MDC. For charged tracks, the distance of closest approach to the interaction point (IP) must be less than 10 cm along the z axis, and less than 1 cm in the transverse plane. The number of charged tracks is required to be two. Particle identification (PID) for charged tracks combines measurements of the dE/dx in the MDC and the flight time in the TOF to form likelihoods $\mathcal{L}(h)(h = p, K, \pi)$ for each hadron h hypothesis. For $h_c \to \pi^+\pi^-\pi^0$ and $h_c \to \pi^+\pi^-\eta$, the charged pions are required to satisfy $\mathcal{L}(\pi) > \mathcal{L}(K)$ and $\mathcal{L}(\pi) > \mathcal{L}(p)$, while for $h_c \to K^+K^-\pi^0$ and $h_c \to K^+K^-\eta$, the kaons are required to satisfy $\mathcal{L}(K) > \mathcal{L}(\pi)$ and $\mathcal{L}(K) > \mathcal{L}(p)$.

Photon candidates are identified using showers in the EMC. The deposited energy of each shower must be more than 25 MeV in the barrel region ($|\cos\theta| < 0.80$) and more than 50 MeV in the end cap region ($0.86 < |\cos\theta| < 0.92$). To exclude showers that originate from charged tracks, the angle subtended by the EMC shower and the position of the closest charged track at the EMC must be greater than 10 degrees as measured from the IP. To suppress electronic noise and showers unrelated to the event, the difference between the EMC time and the event start time is required to be within [0, 700] ns.

The π^0 and η candidates are reconstructed from $\gamma\gamma$ combinations with invariant mass windows in $(0.08, 0.20)$ GeV/c^2 and $(0.45, 0.65)$ GeV/c^2, respectively. The invariant mass of $\gamma\gamma$ is then constrained to the known mass of π^0 or η [6] via a one-constraint (1C) kinematic fit requiring $\chi^2_{1C} < 200$.

To suppress background and improve the mass resolution, a six-constraint (6C) kinematic fit, including the total initial four-momentum of the colliding beams, an invariant mass constraint of π^0 decaying from $\psi(3686)$, and an invariant mass constraint of π^0 or η decaying from h_c, is performed according to the final states of each decay mode. The best $\pi^+\pi^-(K^+K^-)\pi^0\pi^0$ or $\pi^+\pi^-(K^+K^-)\pi^0\eta$ combination is selected with a minimum χ^2_{6C} if there is more than one. The requirement applied to χ^2_{6C} is optimized using the Punzi figure of merit (FOM) $\frac{\epsilon}{a/2+\sqrt{B}}$ [28], where ϵ is signal efficiency, $a = 5$ stands for the expected significance level, and B represents the number of expected background events, estimated with the inclusive MC sample.

Considering the background events with three or five photons versus our signal events with four photons, the $\chi^2_{4C,n\gamma}$ ($n = 3$, 4, 5) values from a four-constraint (4C) kinematic fit together with three, four, and five photons are obtained. We require $\chi^2_{4C,4\gamma} < \chi^2_{4C,3\gamma}$ and $\chi^2_{4C,4\gamma} < \chi^2_{4C,5\gamma}$ for modes II, III, and IV. For mode I, only $\chi^2_{4C,4\gamma} < \chi^2_{4C,3\gamma}$ is applied to improve the ratio of signal to noise. Another prominent background that originates from the decay of $\psi(3686) \to \pi^0\pi^0 J/\psi$ or $\psi(3686) \to \eta J/\psi$ is vetoed by the requirement on the $\pi^0\pi^0$ or η recoil mass $\sqrt{(p_{\psi(3686)} - p_{\pi^0\pi^0/\eta})^2}$ to be outside the J/ψ signal window, where $p_{\psi(3686)}$ is the $\psi(3686)$ four momentum, and $p_{\pi^0\pi^0/\eta}$ is the $\pi^0\pi^0$ or η four momentum. When the final states include π^0, the momentum of π^0 from $\psi(3686) \to \pi^0 h_c$ is usually lower than that from h_c decay. The former and latter π^0s are tagged as π^0_L and π^0_H, respectively. Furthermore, events containing resonances formed with the π^0_L are regarded as background events. These background events are vetoed with additional selection criteria, especially for $\omega \to \pi^+\pi^-\pi^0_L$, $f_0(980) \to \pi^0_L\pi^0_H$, and $K^*(892)^\pm \to K^\pm\pi^0_L$. By combining one photon from π^0 decay and the other from η decay, fake $\gamma\gamma$ combinations from π^0 decay are removed by the requirement on the invariant mass of $\gamma\gamma$ in the $h_c \to K^+K^-\eta$ decay. The above-mentioned requirements on the J/ψ mass window for mode I, M($\pi^+\pi^-\pi^0_L$), M($\pi^0_L\pi^0_H$), M($K^\pm\pi^0_L$), and M($\gamma\gamma$) are also optimized using the FOM. Finally, the background events from $\psi(3686) \to \pi^0\pi^0 J/\psi, J/\psi \to \mu^+\mu^-$ with $\mu^+\mu^-$ misidentified as $\pi^+\pi^-$ are vetoed by requiring a certain penetration depth in the MUC. All detailed selection criteria are listed in Table I.

After applying all the selection criteria, the remaining backgrounds from the inclusive MC sample are analyzed

TABLE I.   Applied requirements on the χ^2_{6C}, invariant mass (M) windows, and recoil mass (RM) windows used as vetoes in each decay. Here, m denotes the known particle mass [6].

Mode	χ^2_{6C}	Veto
I	<30	$\|\text{RM}(\pi^0\pi^0) - m_{J/\psi}\| > 72 \text{ MeV}/c^2$
		$\|\text{M}(\pi^+\pi^-\pi^0_L) - m_\omega\| > 28 \text{ MeV}/c^2$
		Depth of $\mu^\pm < 40$ cm
II	<50	$\|\text{RM}(\pi^0\pi^0) - m_{J/\psi}\| > 20 \text{ MeV}/c^2$
		$\|\text{M}(\pi^0_L\pi^0_H) - m_{f_0(980)}\| > 110 \text{ MeV}/c^2$
		$\|\text{M}(K^\pm\pi^0_L) - m_{K^*(892)^\pm}\| > 40 \text{ MeV}/c^2$
III	<35	$\|\text{RM}(\eta) - m_{J/\psi}\| > 10 \text{ MeV}/c^2$
		$\|\text{M}(\gamma\gamma) - m_{\pi^0}\| > 5 \text{ MeV}/c^2$
		$\|\text{M}(K^\pm\pi^0_L) - m_{K^*(892)^\pm}\| > 15 \text{ MeV}/c^2$
IV	<24	$\|\text{RM}(\eta) - m_{J/\psi}\| > 10 \text{ MeV}/c^2$
		Depth of $\mu^\pm < 35$ cm

by the TOPOANA [29] package. These background events mostly have the same final states as the signal events and are difficult to suppress. The background from the continuum production is estimated with the data sample taken at the center-of-mass energy of 3.650 GeV, with an integrated luminosity of 410 pb^{-1}. The surviving events do not contribute to the peak position of h_c, i.e., the distributions of the selected h_c candidates from the continuum production and the inclusive MC sample are smooth.

IV. EXTRACTION OF SIGNAL YIELDS

To determine the number of signal events N_{sig} in each decay, unbinned maximum likelihood fits are performed to the invariant mass spectra as shown in Fig 1. In the fit, the h_c signal is described by an MC-simulated shape convolved with a free-parameter Gaussian function accounting for the mass resolution difference between data and MC simulation. The mass resolution estimated from MC simulation is around 1.2 MeV/c^2 for each h_c decay channel. The background shape is represented by an ARGUS function [30], with the endpoint set to the kinematic threshold of 3.551 GeV/c^2.

The branching fraction of each signal decay is determined by

$$\mathcal{B}(h_c \to h^+h^-\pi^0/\eta) = \frac{N_{\text{sig}}}{N_{\psi(3686)} \cdot \prod_i \mathcal{B}_i \cdot \epsilon}, \quad (1)$$

where N_{sig} stands for the number of signal events obtained from the fit; $N_{\psi(3686)}$ represents the total number of $\psi(3686)$ events [11], $\prod_i \mathcal{B}_i = \mathcal{B}(\psi(3686) \to \pi^0 h_c) \cdot \mathcal{B}(\pi^0 \to \gamma\gamma) \cdot \mathcal{B}(\pi^0/\eta \to \gamma\gamma)$, where $\mathcal{B}(\psi(3686) \to \pi^0 h_c)$ is the branching fraction of $\psi(3686) \to \pi^0 h_c$, and
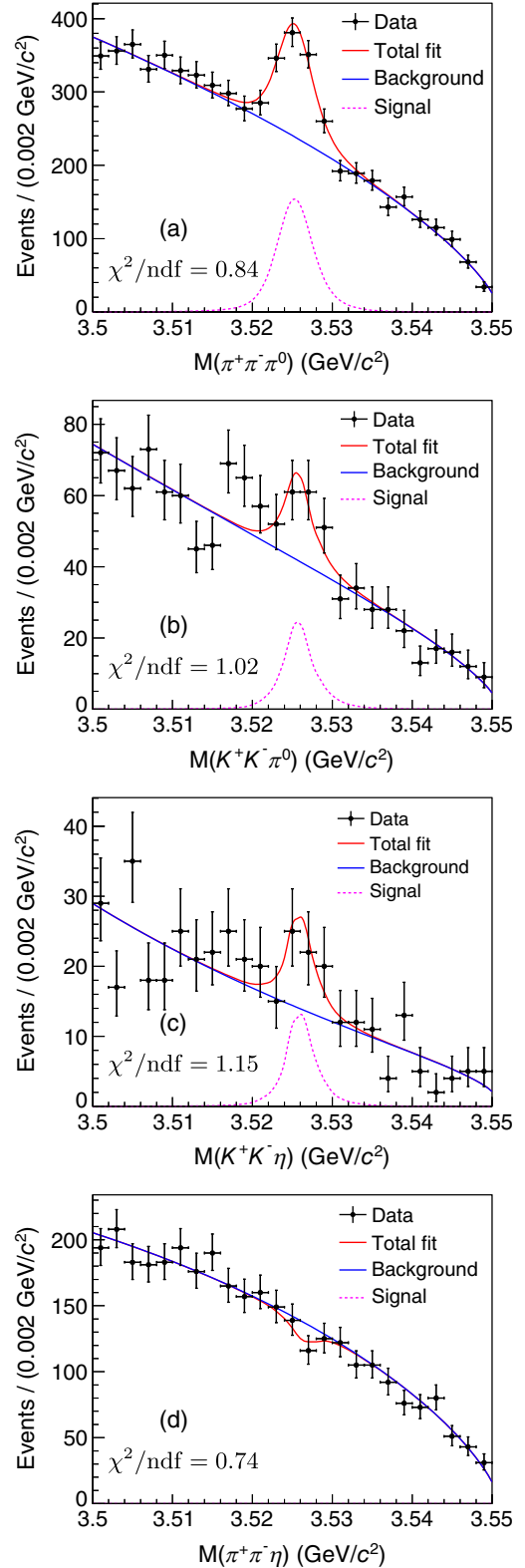

FIG. 1. The fits to the invariant mass distributions for (a) $h_c \to \pi^+\pi^-\pi^0$, (b) $h_c \to K^+K^-\pi^0$, (c) $h_c \to K^+K^-\eta$, and (d) $h_c \to \pi^+\pi^-\eta$. The black dots with error bars are the data, the red solid lines represent the fit results, the blue solid lines indicate the backgrounds, and the pink dashed lines illustrate the signals.
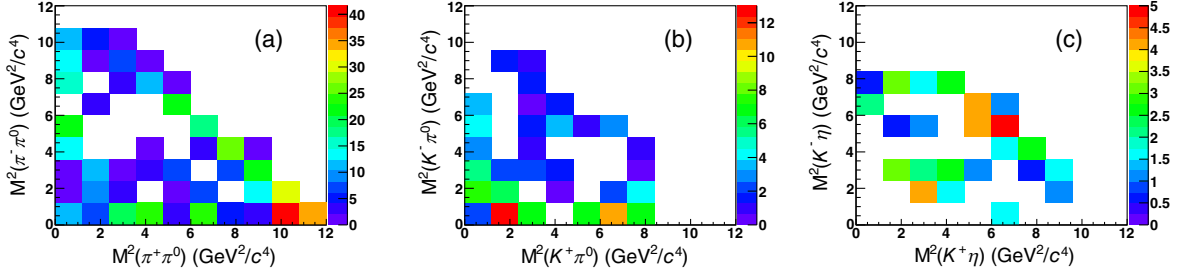
FIG. 2.   Dalitz plots of data with the background events subtracted for (a) $h_c \to \pi^+\pi^-\pi^0$, (b) $h_c \to K^+K^-\pi^0$, and (c) $h_c \to K^+K^-\eta$.

$\mathcal{B}(\pi^0 \to \gamma\gamma) \cdot \mathcal{B}(\pi^0/\eta \to \gamma\gamma)$ is the product of the branching fractions. These branching fractions are quoted from the PDG [6].

For each signal decay, we obtain the Dalitz plot of $M^2(h^+\pi^0/\eta)$ versus $M^2(h^-\pi^0/\eta)$ in the $h_c \to h^+h^-\pi^0/\eta$ signal region defined as $3.52 < M(h^+h^-\pi^0/\eta) < 3.53\,\mathrm{GeV}/c^2$ from data, where the background events have been subtracted using the normalized h_c sidebands defined as $(3.505, 3.515)\,\mathrm{GeV}/c^2$ or $(3.535, 3.545)\,\mathrm{GeV}/c^2$. The corresponding Dalitz plots are shown in Fig. 2, where we divide the Dalitz plot of data into 10×10 bins, with a bin size of $1.2\,\mathrm{GeV}^2/c^4$. Due to limited statistics, no intermediate resonances are found. The detection efficiencies are obtained from signal MC simulation, corrected by the Dalitz plots observed in data for modes I, II, and III as follows. The corrected efficiencies are determined via

$$\epsilon = \frac{\sum_i s_i \cdot \epsilon_i}{S}, \qquad (2)$$

where i runs over all bins, s_i and ϵ_i are the number of signal candidates in data and the efficiency from MC events for the ith bin, and S is the total number of h_c signal candidates in data. The efficiencies are 17.7%, 9.7%, 13.1%, and 14.2% for modes I, II, III, and IV, respectively.

The statistical significance is estimated from the difference of the logarithmic likelihoods of the fits without and with a signal component with the difference in the number of degrees of freedom ($\Delta_{\mathrm{ndf}} = 3$) that are considered. The significance of mode I is 10.8σ and the evidences for the decay modes II and III are found with statistical significances of 3.5σ and 3.3σ, respectively. After considering systematic effects, the resulting significances are 9.6σ,

3.5σ, and 3.3σ for modes I, II, and III respectively. Since no obvious signal of mode IV is observed, assuming that the number of signal events follows a Poisson distribution with a uniform prior probability density function, a Bayesian upper limit [31] of mode IV (accounting for systematic uncertainties) is determined. The obtained results for the four studied modes are listed in Table II.

V. SYSTEMATIC UNCERTAINTIES

In the branching fraction measurements, the systematic uncertainties are divided into multiplicative and additive terms. The multiplicative terms include tracking, PID, π^0 and η reconstruction, kinematic fit, selection criteria, number of $\psi(3686)$ events, and quoted branching fractions. The additive terms originate from fit range, signal shape, and background shape in the fit procedure.

The tracking efficiency is estimated with the control samples of $J/\psi \to p\bar{p}\pi^+\pi^-$ [32] and $e^+e^- \to \pi^+\pi^-K^+K^-$ [33]. The resulting systematic uncertainty on the branching fraction due to the tracking is assigned to be 1.0% for each charged pion or kaon. The uncertainties due to the PID for charged pion and kaon are studied with the control samples of $J/\psi \to \pi^+\pi^-\pi^0$ and $J/\psi \to K^+K^-\pi^0$ [34], and are assigned to be 1.0% for each pion or kaon.

The systematic uncertainty of the π^0 reconstruction is estimated using the control samples of $\psi(3686) \to \pi^0\pi^0 J/\psi$ and $e^+e^- \to \omega\pi^0$, resulting in the uncertainty as a function of π^0 momentum. The systematic uncertainties in the π^0 reconstruction are assigned according to the momentum of π^0 in the final state, which are 5.5%, 5.2%, 1.0%, and 1.0% for the decay modes I, II, III, and IV, respectively. The systematic uncertainty of the η

TABLE II.   The branching fractions (or their upper limit at 90% confidence level) for each h_c decay together with the corrected detection efficiencies, the fitted signal yields, and the signal significances with systematic uncertainties included. The first uncertainties are statistical, the second are systematic.

Mode	$\epsilon(\%)$	Signal yield	Signal significance	$\mathcal{B}$ [This work]	$\mathcal{B}$ [PDG] [6]
I	17.7	472 ± 56	9.6σ	$(1.36 \pm 0.16 \pm 0.14) \times 10^{-3}$	$(1.9 \pm 0.5) \times 10^{-3}$
II	9.7	62 ± 16	3.5σ	$(3.26 \pm 0.84 \pm 0.36) \times 10^{-4}$	$<6 \times 10^{-4}$
III	13.1	32 ± 11	3.3σ	$(3.13 \pm 1.08 \pm 0.38) \times 10^{-4}$	$<1.0 \times 10^{-3}$
IV	14.2	<44.5	$\cdots$	$<4.0 \times 10^{-4}$	$\cdots$

reconstruction is estimated to be 1.0% using a high purity control sample of $J/\psi \to p\bar{p}\eta$ [35]. Since the uncertainties between two π^0s or between π^0 and η are assumed to be correlated, their values are added linearly.

The systematic uncertainties associated with the 6C kinematic fit are assigned as the differences between the efficiencies before and after the helix correction [36], which are 0.6%, 1.0%, 0.9%, and 0.9% for modes I, II, III, and IV, respectively.

A Barlow test [37] is performed to evaluate the uncertainty from the mass window requirements. The significant deviation ζ is defined as

$$\zeta = \frac{|\mathcal{B}_{\text{nominal}} - \mathcal{B}_{\text{test}}|}{\sqrt{|\sigma_{\mathcal{B}_{\text{nominal}}}^2 - \sigma_{\mathcal{B}_{\text{test}}}^2|}}, \tag{3}$$

where $\mathcal{B}$ represents the branching fractions and $\sigma_{\mathcal{B}}^2$ is the statistical uncertainty of $\mathcal{B}$. To obtain the ζ distributions, we examine the branching fractions after enlarging or shrinking the veto region. For different background vetoes, we vary the corresponding mass windows several times with a step of 1 MeV/c^2. Since there is no obvious change larger than 1.0σ for each requirement, we do not assign a systematic uncertainty to this term.

The uncertainty of the total number of $\psi(3686)$ events in data is 0.5% [11]. In the branching fraction calculations, the $\mathcal{B}(\psi(3686) \to \pi^0 h_c)$, $\mathcal{B}(\pi^0 \to \gamma\gamma)$, and $\mathcal{B}(\eta \to \gamma\gamma)$ are quoted from PDG. The total uncertainty due to these quoted branching fractions, which is dominated by $\mathcal{B}(\psi(3686) \to \pi^0 h_c)$, is 5.5% [6,38].

The additive systematic uncertainties are estimated below. The uncertainties due to the fit range are estimated by enlarging or shrinking the nominal fit range of $(3.50, 3.55)$ GeV/c^2 to be $(3.49, 3.55)$ GeV/c^2 and $(3.51, 3.55)$ GeV/c^2. The differences of the fitted signal yields between the nominal and alternative results are taken as the systematic uncertainties. In the nominal fits, the signals are described by the MC-simulated shape convolved with a free-parameter Gaussian function. Since the numbers of signal events are limited for the decay modes II, III, and IV, the uncertainty from the mass resolution difference between data and MC simulation is estimated by changing the standard deviation of the Gaussian function to 1 MeV/c^2, which is determined from the $h_c \to \pi^+\pi^-\pi^0$ model. The differences relative to the nominal fits are taken as the systematic uncertainties. The uncertainties due to the background shape are considered by changing the nominal ARGUS background shape to a second-order Chebyshev polynomial function. The differences in the fitted signal yields are taken as the systematic uncertainties.

When the upper limit of the number of signal events in mode IV is determined, the additive systematic uncertainties are considered by retaining the largest upper limit by a maximum-likelihood fit with different fit ranges, signal

TABLE III. The relative systematic uncertainties (%) on the branching fraction measurements. In mode IV, there are no systematic uncertainties of the efficiency correction and fit procedure due to no evidence for a signal in the data. The uncertainty due to the fit procedure is additive, the others are multiplicative.

Source/Mode	I	II	III	IV
Tracking	2.0	2.0	2.0	2.0
PID	2.0	2.0	2.0	2.0
Reconstruction of π^0 and η	5.5	5.2	2.0	2.0
Kinematic fit	0.6	1.0	0.9	0.9
$N_{\psi(3686)}$	0.5	0.5	0.5	0.5
$\mathcal{B}(\psi(3686) \to \pi^0 h_c)$	5.5	5.5	5.5	5.5
Fit procedure	6.6	7.3	10.1	$\cdots$
Sum	10.6	10.9	12.1	6.6

shapes, and background shapes. To incorporate the multiplicative terms, we convolve the likelihood distribution $\mathcal{L}(N_{\text{sig}})$ with the quadratic sum of the multiplicative terms [39,40].

The individual uncertainties are assumed to be independent and added in quadrature to obtain the total systematic uncertainty. In Table III, the multiplicative terms are listed separately, and "Fit procedure" denotes the quadratic sum of the additive terms.

VI. SUMMARY

Using $(2712.4 \pm 14.3) \times 10^6$ $\psi(3686)$ events, the modes $h_c \to \pi^+\pi^-\pi^0$, $h_c \to K^+K^-\pi^0$, and $h_c \to K^+K^-\eta$ are found with significances of 9.6σ, 3.5σ, and 3.3σ, respectively. Their decay branching fractions are determined to be $\mathcal{B}(h_c \to \pi^+\pi^-\pi^0) = (1.36 \pm 0.16 \pm 0.14) \times 10^{-3}$, $\mathcal{B}(h_c \to K^+K^-\pi^0) = (3.26 \pm 0.84 \pm 0.36) \times 10^{-4}$, and $\mathcal{B}(h_c \to K^+K^-\eta) = (3.13 \pm 1.08 \pm 0.38) \times 10^{-4}$, where the first uncertainties are statistical and the second are systematic. These results are consistent with the PDG values [6], as summarized in Table II. No obvious signal of $h_c \to \pi^+\pi^-\eta$ decay is observed, and the upper limit of its decay branching fraction is determined to be $\mathcal{B}(h_c \to \pi^+\pi^-\eta) < 4.0 \times 10^{-4}$ at 90% confidence level. The isospin conservation in the process $h_c \to K\bar{K}\pi$ leads to a relationship of $\mathcal{B}(h_c \to K^+K^-\pi^0) : \mathcal{B}(h_c \to K^0K^-\pi^+) : \mathcal{B}(h_c \to \bar{K}^0K^+\pi^-) : \mathcal{B}(h_c \to K^0\bar{K}^0\pi^0) = 1 : 2 : 2 : 1$. The $\mathcal{B}(h_c \to K\bar{K}\pi) = (0.20 \pm 0.05)\%$ extrapolated in this work is consistent with that obtained via the $h_c \to K_S^0 K^+\pi^-$ decay mode [41]. Theoretically, $\mathcal{B}(h_c \to K\bar{K}\pi)$ is predicted to be $(1.4 \pm 0.9)\%$ for pQCD or $(5.5 \pm 3.3)\%$ for NRQCD [10]. Since the large uncertainty mainly arises from the input values of $\mathcal{B}(\eta_c \to K\bar{K}\pi)$ and $\Gamma(\eta_c)$ quoted from PDG 2000 [42], we take the most recent results from the PDG [6] and reweigh the $\mathcal{B}(h_c \to K\bar{K}\pi)$ in Ref. [10]. The branching fraction of $h_c \to K\bar{K}\pi$ is calculated to be $(4.4 \pm 0.8)\%$ with pQCD or $(16.9 \pm 7.3)\%$ with NRQCD, which strongly deviates from the experimental results. Since only the

leading-order terms are evaluated in the theoretical calculations from both pQCD and NRQCD, higher precision from theory is desirable.

ACKNOWLEDGMENTS

[1] P. Rubin *et al.* (CLEO Collaboration), Phys. Rev. D **72**, 092004 (2005).

[2] J. L. Rosner *et al.* (CLEO Collaboration), Phys. Rev. Lett. **95**, 102003 (2005).

[3] M. Andreotti *et al.* (Fermilab E835 Collaboration), Phys. Rev. D **72**, 032001 (2005).

[4] S. Dobbs *et al.* (CLEO Collaboration), Phys. Rev. Lett. **101**, 182003 (2008).

[5] M. Ablikim *et al.* (BESIII Collaboration), Phys. Rev. Lett. **104**, 132002 (2010).

[6] R. L. Workman *et al.* (Particle Data Group), Prog. Theor. Exp. Phys. **2022**, 083C01 (2022).

[7] M. Ablikim *et al.* (BESIII Collaboration), Phys. Rev. D **99**, 072008 (2019).

[8] M. Ablikim *et al.* (BESIII Collaboration), Phys. Rev. D **102**, 112007 (2020).

[9] M. Ablikim *et al.* (BESIII Collaboration), Phys. Rev. D **109**, 072018 (2024).

[10] Y. P. Kuang, Phys. Rev. D **65**, 094024 (2002).

[11] M. Ablikim *et al.* (BESIII Collaboration), Chin. Phys. C **48**, 093001 (2024).

[12] M. Ablikim *et al.*, Nucl. Instrum. Methods Phys. Res., Sect. A **614**, 345 (2010).

[13] C. X. Yu *et al.*, *Proceedings of IPAC* (2016), 10.18429/JACoW-IPAC2016-TUYA01.

[14] M. Ablikim *et al.*, Chin. Phys. C **44**, 040001 (2020).

[15] J. Lu, Y. Xiao, and X. Ji, Radiat. Detect. Technol. Methods **4**, 337 (2020).

[16] J. Zhang *et al.*, Radiat. Detect. Technol. Methods **6**, 289 (2022).

[17] X. Li *et al.*, Radiat. Detect. Technol. Methods **1**, 13 (2017).

[18] Y. X. Guo, S. S. Sen, F. F. An, Y. R. Xing, Z. Ming, Z. Wu, H. L. Dai, H. Y. Kun, L. Cheng, Z. Y. Deng, H. M. Liu, and L. W. Guo, Radiat. Detect. Technol. Methods **1**, 15 (2017).

[19] P. Cao *et al.*, Nucl. Instrum. Methods Phys. Res., Sect. A **953**, 163053 (2020).

[20] S. Agostinelli *et al.*, Nucl. Instrum. Methods Phys. Res., Sect. A **506**, 250 (2003).

[21] S. Jadach, B. Ward, and Z. Wąs, Comput. Phys. Commun. **130**, 260 (2000).

[22] S. Jadach, B. Ward, and Z. Wąs, Phys. Rev. D **63**, 113009 (2001).

[23] D. J. Lange, Nucl. Instrum. Methods Phys. Res., Sect. A **462**, 152 (2001).

[24] R. G. Ping, Chin. Phys. C **32**, 599 (2008).

[25] J. C. Chen, G. S. Huang, X. R. Qi, D. H. Zhang, and Y. S. Zhu, Phys. Rev. D **62**, 034003 (2000).

[26] R. L. Yang, R. G. Ping, and H. Chen, Chin. Phys. Lett. **31**, 061301 (2014).

[27] P. Golonka and Z. Wąs, Eur. Phys. J. C **45**, 97 (2006).

[28] G. Punzi, eConf C **030908**, MODT002 (2003), arXiv:physics/0308063.

[29] X. Y. Zhou, S. X. Du, G. Li, and C. P. Shen, Comput. Phys. Commun. **258**, 107540 (2021).

[30] H. Albrecht *et al.* (ARGUS Collaboration), Phys. Lett. B **241**, 278 (1990).

[31] G. J. Feldman and R. D. Cousins, Phys. Rev. D **57**, 3873 (1998).

[32] W. L. Yuan, X. C. Ai, X. B. Ji, S. J. Chen, Y. Zhang, W. L. Hui, L. L. Wang, and Y. Yuan, Chin. Phys. C **40**, 026201 (2016).

[33] M. Ablikim *et al.* (BESIII Collaboration), Phys. Rev. D **99,** 091103 (2019).

[34] M. Ablikim *et al.* (BESIII Collaboration), Phys. Rev. D **83,** 112005 (2011).

[35] M. Ablikim *et al.* (BESIII Collaboration), Phys. Rev. D **81,** 052005 (2010).

[36] M. Ablikim *et al.* (BESIII Collaboration), Phys. Rev. D **87,** 012002 (2013).

[37] R. Barlow, arXiv:hep-ex/0207026.

[38] M. Ablikim *et al.* (BESIII Collaboration), Phys. Rev. D **106,** 072007 (2022).

[39] K. Stenson, arXiv:physics/0605236.

[40] X. X. Liu, X. R. Lyu, and Y. S. Zhu, Chin. Phys. C **39,** 103001 (2015).

[41] M. Ablikim *et al.* (BESIII Collaboration), Phys. Rev. D **110,** 012007 (2024).

[42] D. E. Groom *et al.* (Particle Data Group), Eur. Phys. J. C **15,** 1 (2000).

M. Ablikim,[1] M. N. Achasov,[4,c] P. Adlarson,[76] O. Afedulidis,[3] X. C. Ai,[81] R. Aliberti,[35] A. Amoroso,[75a,75c] Q. An,[72,58,a] Y. Bai,[57] O. Bakina,[36] I. Balossino,[29a] Y. Ban,[46,h] H.-R. Bao,[64] V. Batozskaya,[1,44] K. Begzsuren,[32] N. Berger,[35] M. Berlowski,[44] M. Bertani,[28a] D. Bettoni,[29a] F. Bianchi,[75a,75c] E. Bianco,[75a,75c] A. Bortone,[75a,75c] I. Boyko,[36] R. A. Briere,[5] A. Brueggemann,[69] H. Cai,[77] X. Cai,[1,58] A. Calcaterra,[28a] G. F. Cao,[1,64] N. Cao,[1,64] S. A. Cetin,[62a] J. F. Chang,[1,58] G. R. Che,[43] G. Chelkov,[36,b] C. Chen,[43] C. H. Chen,[9] Chao Chen,[55] G. Chen,[1] H. S. Chen,[1,64] H. Y. Chen,[20] M. L. Chen,[1,58,64] S. J. Chen,[42] S. L. Chen,[45] S. M. Chen,[61] T. Chen,[1,64] X. R. Chen,[31,64] X. T. Chen,[1,64] Y. B. Chen,[1,58] Y. Q. Chen,[34] Z. J. Chen,[25,i] Z. Y. Chen,[1,64] S. K. Choi,[10] G. Cibinetto,[29a] F. Cossio,[75c] J. J. Cui,[50] H. L. Dai,[1,58] J. P. Dai,[79] A. Dbeyssi,[18] R. E. de Boer,[3] D. Dedovich,[36] C. Q. Deng,[73] Z. Y. Deng,[1] A. Denig,[35] I. Denysenko,[36] M. Destefanis,[75a,75c] F. De Mori,[75a,75c] B. Ding,[67,1] X. X. Ding,[46,h] Y. Ding,[40] Y. Ding,[34] J. Dong,[1,58] L. Y. Dong,[1,64] M. Y. Dong,[1,58,64] X. Dong,[77] M. C. Du,[1] S. X. Du,[81] Y. Y. Duan,[55] Z. H. Duan,[42] P. Egorov,[36,b] Y. H. Fan,[45] J. Fang,[59] J. Fang,[1,58] S. S. Fang,[1,64] W. X. Fang,[1] Y. Fang,[1] Y. Q. Fang,[1,58] R. Farinelli,[29a] L. Fava,[75b,75c] F. Feldbauer,[3] G. Felici,[28a] C. Q. Feng,[72,58] J. H. Feng,[59] Y. T. Feng,[72,58] M. Fritsch,[3] C. D. Fu,[1] J. L. Fu,[64] Y. W. Fu,[1,64] H. Gao,[64] X. B. Gao,[41] Y. N. Gao,[46,h] Yang Gao,[72,58] S. Garbolino,[75c] I. Garzia,[29a,29b] L. Ge,[81] P. T. Ge,[19] Z. W. Ge,[42] C. Geng,[59] E. M. Gersabeck,[68] A. Gilman,[70] K. Goetzen,[13] L. Gong,[40] W. X. Gong,[1,58] W. Gradl,[35] S. Gramigna,[29a,29b] M. Greco,[75a,75c] M. H. Gu,[1,58] Y. T. Gu,[15] C. Y. Guan,[1,64] A. Q. Guo,[31,64] L. B. Guo,[41] M. J. Guo,[50] R. P. Guo,[49] Y. P. Guo,[12,g] A. Guskov,[36,b] J. Gutierrez,[27] K. L. Han,[64] T. T. Han,[1] F. Hanisch,[3] X. Q. Hao,[19] F. A. Harris,[66] K. K. He,[55] K. L. He,[1,64] F. H. Heinsius,[3] C. H. Heinz,[35] Y. K. Heng,[1,58,64] C. Herold,[60] T. Holtmann,[3] P. C. Hong,[34] G. Y. Hou,[1,64] X. T. Hou,[1,64] Y. R. Hou,[64] Z. L. Hou,[1] B. Y. Hu,[59] H. M. Hu,[1,64] J. F. Hu,[56,j] S. L. Hu,[12,g] T. Hu,[1,58,64] Y. Hu,[1] G. S. Huang,[72,58] K. X. Huang,[59] L. Q. Huang,[31,64] X. T. Huang,[50] Y. P. Huang,[1] Y. S. Huang,[59] T. Hussain,[74] F. Hölzken,[3] N. Hüsken,[35] N. in der Wiesche,[69] J. Jackson,[27] S. Janchiv,[32] J. H. Jeong,[10] Q. Ji,[1] Q. P. Ji,[19] W. Ji,[1,64] X. B. Ji,[1,64] X. L. Ji,[1,58] Y. Y. Ji,[50] X. Q. Jia,[50] Z. K. Jia,[72,58] D. Jiang,[1,64] H. B. Jiang,[77] P. C. Jiang,[46,h] S. S. Jiang,[39] T. J. Jiang,[16] X. S. Jiang,[1,58,64] Y. Jiang,[64] J. B. Jiao,[50] J. K. Jiao,[34] Z. Jiao,[23] S. Jin,[42] Y. Jin,[67] M. Q. Jing,[1,64] X. M. Jing,[64] T. Johansson,[76] S. Kabana,[33] N. Kalantar-Nayestanaki,[65] X. L. Kang,[9] X. S. Kang,[40] M. Kavatsyuk,[65] B. C. Ke,[81] V. Khachatryan,[27] A. Khoukaz,[69] R. Kiuchi,[1] O. B. Kolcu,[62a] B. Kopf,[3] M. Kuessner,[3] X. Kui,[1,64] N. Kumar,[26] A. Kupsc,[44,76] W. Kühn,[37] J. J. Lane,[68] L. Lavezzi,[75a,75c] T. T. Lei,[72,58] Z. H. Lei,[72,58] M. Lellmann,[35] T. Lenz,[35] C. Li,[47] C. Li,[43] C. H. Li,[39] Cheng Li,[72,58] D. M. Li,[81] F. Li,[1,58] G. Li,[1] H. B. Li,[1,64] H. J. Li,[19] H. N. Li,[56,j] Hui Li,[43] J. R. Li,[61] J. S. Li,[59] K. Li,[1] K. L. Li,[19] L. J. Li,[1,64] L. K. Li,[1] Lei Li,[48] M. H. Li,[43] P. R. Li,[38,k,l] Q. M. Li,[1,64] Q. X. Li,[50] R. Li,[17,31] S. X. Li,[12] T. Li,[50] W. D. Li,[1,64] W. G. Li,[1,a] X. Li,[1,64] X. H. Li,[72,58] X. L. Li,[50] X. Y. Li,[1,64] X. Z. Li,[59] Y. G. Li,[46,h] Z. J. Li,[59] Z. Y. Li,[79] C. Liang,[42] H. Liang,[1,64] H. Liang,[72,58] Y. F. Liang,[54] Y. T. Liang,[31,64] G. R. Liao,[14] Y. P. Liao,[1,64] J. Libby,[26] A. Limphirat,[60] C. C. Lin,[55] D. X. Lin,[31,64] T. Lin,[1] B. J. Liu,[1] B. X. Liu,[77] C. Liu,[34] C. X. Liu,[1] F. Liu,[1] F. H. Liu,[53] Feng Liu,[6] G. M. Liu,[56,j] H. Liu,[38,k,l] H. B. Liu,[15] H. H. Liu,[1] H. M. Liu,[1,64] Huihui Liu,[21] J. B. Liu,[72,58] J. Y. Liu,[1,64] K. Liu,[38,k,l] K. Y. Liu,[40] Ke Liu,[22] L. Liu,[72,58] L. C. Liu,[43] Lu Liu,[43] M. H. Liu,[12,g] P. L. Liu,[1] Q. Liu,[64] S. B. Liu,[72,58] T. Liu,[12,g] W. K. Liu,[43] W. M. Liu,[72,58] X. Liu,[38,k,l] X. Liu,[39] Y. Liu,[81] Y. Liu,[38,k,l] Y. B. Liu,[43] Z. A. Liu,[1,58,64] Z. D. Liu,[9] Z. Q. Liu,[50] X. C. Lou,[1,58,64] F. X. Lu,[59] H. J. Lu,[23] J. G. Lu,[1,58] X. L. Lu,[1] Y. Lu,[7] Y. P. Lu,[1,58] Z. H. Lu,[1,64] C. L. Luo,[41] J. R. Luo,[59] M. X. Luo,[80] T. Luo,[12,g] X. L. Luo,[1,58] X. R. Lyu,[64] Y. F. Lyu,[43] F. C. Ma,[40] H. Ma,[79] H. L. Ma,[1] J. L. Ma,[1,64] L. L. Ma,[50] L. R. Ma,[67] M. M. Ma,[1,64] Q. M. Ma,[1] R. Q. Ma,[1,64] T. Ma,[72,58] X. T. Ma,[1,64] X. Y. Ma,[1,58] Y. Ma,[46,h] Y. M. Ma,[31] F. E. Maas,[18] M. Maggiora,[75a,75c] S. Malde,[70] Y. J. Mao,[46,h] Z. P. Mao,[1] S. Marcello,[75a,75c] Z. X. Meng,[67] J. G. Messchendorp,[13,65] G. Mezzadri,[29a] H. Miao,[1,64] T. J. Min,[42] R. E. Mitchell,[27] X. H. Mo,[1,58,64] B. Moses,[27] N. Yu. Muchnoi,[4,c] J. Muskalla,[35] Y. Nefedov,[36] F. Nerling,[18,e] L. S. Nie,[20] I. B. Nikolaev,[4,c] Z. Ning,[1,58] S. Nisar,[11,m]

Q. L. Niu,[38,k,l] W. D. Niu,[55] Y. Niu,[50] S. L. Olsen,[64] Q. Ouyang,[1,58,64] S. Pacetti,[28b,28c] X. Pan,[55] Y. Pan,[57] A. Pathak,[34] Y. P. Pei,[72,58] M. Pelizaeus,[3] H. P. Peng,[72,58] Y. Y. Peng,[38,k,l] K. Peters,[13,e] J. L. Ping,[41] R. G. Ping,[1,64] S. Plura,[35] V. Prasad,[33] F. Z. Qi,[1] H. Qi,[72,58] H. R. Qi,[61] M. Qi,[42] T. Y. Qi,[12,g] S. Qian,[1,58] W. B. Qian,[64] C. F. Qiao,[64] X. K. Qiao,[81] J. J. Qin,[73] L. Q. Qin,[14] L. Y. Qin,[72,58] X. P. Qin,[12,g] X. S. Qin,[50] Z. H. Qin,[1,58] J. F. Qiu,[1] Z. H. Qu,[73] C. F. Redmer,[35] K. J. Ren,[39] A. Rivetti,[75c] M. Rolo,[75c] G. Rong,[1,64] Ch. Rosner,[18] S. N. Ruan,[43] N. Salone,[44] A. Sarantsev,[36,d] Y. Schelhaas,[35] K. Schoenning,[76] M. Scodeggio,[29a] K. Y. Shan,[12,g] W. Shan,[24] X. Y. Shan,[72,58] Z. J. Shang,[38,k,l] J. F. Shangguan,[16] L. G. Shao,[1,64] M. Shao,[72,58] C. P. Shen,[12,g] H. F. Shen,[1,8] W. H. Shen,[64] X. Y. Shen,[1,64] B. A. Shi,[64] H. Shi,[72,58] H. C. Shi,[72,58] J. L. Shi,[12,g] J. Y. Shi,[1] Q. Q. Shi,[55] S. Y. Shi,[73] X. Shi,[1,58] J. J. Song,[19] T. Z. Song,[59] W. M. Song,[34,1] Y. J. Song,[12,g] Y. X. Song,[46,h,n] S. Sosio,[75a,75c] S. Spataro,[75a,75c] F. Stieler,[35] S. S. Su,[40] Y. J. Su,[64] G. B. Sun,[77] G. X. Sun,[1] H. Sun,[64] H. K. Sun,[1] J. F. Sun,[19] K. Sun,[61] L. Sun,[77] S. S. Sun,[1,64] T. Sun,[51,f] W. Y. Sun,[34] Y. Sun,[9] Y. J. Sun,[72,58] Y. Z. Sun,[1] Z. Q. Sun,[1,64] Z. T. Sun,[50] C. J. Tang,[54] G. Y. Tang,[1] J. Tang,[59] M. Tang,[72,58] Y. A. Tang,[77] L. Y. Tao,[73] Q. T. Tao,[25,i] M. Tat,[70] J. X. Teng,[72,58] V. Thoren,[76] W. H. Tian,[59] Y. Tian,[31,64] Z. F. Tian,[77] I. Uman,[62b] Y. Wan,[55] S. J. Wang,[50] B. Wang,[1] B. L. Wang,[64] Bo Wang,[72,58] D. Y. Wang,[46,h] F. Wang,[73] H. J. Wang,[38,k,l] J. J. Wang,[77] J. P. Wang,[50] K. Wang,[1,58] L. L. Wang,[1] M. Wang,[50] N. Y. Wang,[64] S. Wang,[12,g] S. Wang,[38,k,l] T. Wang,[12,g] T. J. Wang,[43] W. Wang,[73] W. Wang,[59] W. P. Wang,[35,58,72,o] X. Wang,[46,h] X. F. Wang,[38,k,l] X. J. Wang,[39] X. L. Wang,[12,g] X. N. Wang,[1] Y. Wang,[61] Y. D. Wang,[45] Y. F. Wang,[1,58,64] Y. L. Wang,[19] Y. N. Wang,[45] Y. Q. Wang,[1] Yaqian Wang,[17] Yi Wang,[61] Z. Wang,[1,58] Z. L. Wang,[73] Z. Y. Wang,[1,64] Ziyi Wang,[64] D. H. Wei,[14] F. Weidner,[69] S. P. Wen,[1] Y. R. Wen,[39] U. Wiedner,[3] G. Wilkinson,[70] M. Wolke,[76] L. Wollenberg,[3] C. Wu,[39] J. F. Wu,[1,8] L. H. Wu,[1] L. J. Wu,[1,64] X. Wu,[12,g] X. H. Wu,[34] Y. Wu,[72,58] Y. H. Wu,[55] Y. J. Wu,[31] Z. Wu,[1,58] L. Xia,[72,58] X. M. Xian,[39] B. H. Xiang,[1,64] T. Xiang,[46,h] D. Xiao,[38,k,l] G. Y. Xiao,[42] S. Y. Xiao,[1] Y. L. Xiao,[12,g] Z. J. Xiao,[41] C. Xie,[42] X. H. Xie,[46,h] Y. Xie,[50] Y. G. Xie,[1,58] Y. H. Xie,[6] Z. P. Xie,[72,58] T. Y. Xing,[1,64] C. F. Xu,[1,64] C. J. Xu,[59] G. F. Xu,[1] H. Y. Xu,[67,2,p] M. Xu,[72,58] Q. J. Xu,[16] Q. N. Xu,[30] W. Xu,[1] W. L. Xu,[67] X. P. Xu,[55] Y. Xu,[40] Y. C. Xu,[78] Z. S. Xu,[64] F. Yan,[12,g] L. Yan,[12,g] W. B. Yan,[72,58] W. C. Yan,[81] X. Q. Yan,[1,64] H. J. Yang,[51,f] H. L. Yang,[34] H. X. Yang,[1] T. Yang,[1] Y. Yang,[12,g] Y. F. Yang,[43] Y. F. Yang,[1,64] Y. X. Yang,[1,64] Z. W. Yang,[38,k,l] Z. P. Yao,[50] M. Ye,[1,58] M. H. Ye,[8] J. H. Yin,[1] Junhao Yin,[43] Z. Y. You,[59] B. X. Yu,[1,58,64] C. X. Yu,[43] G. Yu,[1,64] J. S. Yu,[25,i] M. C. Yu,[40] T. Yu,[73] X. D. Yu,[46,h] Y. C. Yu,[81] C. Z. Yuan,[1,64] J. Yuan,[34] J. Yuan,[45] L. Yuan,[2] S. C. Yuan,[1,64] Y. Yuan,[1,64] Z. Y. Yuan,[59] C. X. Yue,[39] A. A. Zafar,[74] F. R. Zeng,[50] S. H. Zeng,[63a,63b,63c,63d] X. Zeng,[12,g] Y. Zeng,[25,i] Y. J. Zeng,[59] Y. J. Zeng,[1,64] X. Y. Zhai,[34] Y. C. Zhai,[50] Y. H. Zhan,[59] A. Q. Zhang,[1,64] B. L. Zhang,[1,64] B. X. Zhang,[1] D. H. Zhang,[43] G. Y. Zhang,[19] H. Zhang,[72,58] H. Zhang,[81] H. C. Zhang,[1,58,64] H. H. Zhang,[59] H. H. Zhang,[34] H. Q. Zhang,[1,58,64] H. R. Zhang,[72,58] H. Y. Zhang,[1,58] J. Zhang,[81] J. Zhang,[59] J. J. Zhang,[52] J. L. Zhang,[20] J. Q. Zhang,[41] J. S. Zhang,[12,g] J. W. Zhang,[1,58,64] J. X. Zhang,[38,k,l] J. Y. Zhang,[1] J. Z. Zhang,[1,64] Jianyu Zhang,[64] L. M. Zhang,[61] Lei Zhang,[42] P. Zhang,[1,64] Q. Y. Zhang,[34] R. Y. Zhang,[38,k,l] S. H. Zhang,[1,64] Shulei Zhang,[25,i] X. D. Zhang,[45] X. M. Zhang,[1] X. Y. Zhang,[40] X. Y. Zhang,[50] Y. Zhang,[73] Y. Zhang,[1] Y. T. Zhang,[81] Y. H. Zhang,[1,58] Y. M. Zhang,[39] Yan Zhang,[72,58] Z. D. Zhang,[1] Z. H. Zhang,[1] Z. L. Zhang,[34] Z. Y. Zhang,[77] Z. Y. Zhang,[43] Z. Z. Zhang,[45] G. Zhao,[1] J. Y. Zhao,[1,64] J. Z. Zhao,[1,58] L. Zhao,[1] Lei Zhao,[72,58] M. G. Zhao,[43] N. Zhao,[79] R. P. Zhao,[64] S. J. Zhao,[81] Y. B. Zhao,[1,58] Y. X. Zhao,[31,64] Z. G. Zhao,[72,58] A. Zhemchugov,[36,b] B. Zheng,[73] B. M. Zheng,[34] J. P. Zheng,[1,58] W. J. Zheng,[1,64] Y. H. Zheng,[64] B. Zhong,[41] X. Zhong,[59] H. Zhou,[50] J. Y. Zhou,[34] L. P. Zhou,[1,64] S. Zhou,[6] X. Zhou,[77] X. K. Zhou,[6] X. R. Zhou,[72,58] X. Y. Zhou,[39] Y. Z. Zhou,[12,g] Z. C. Zhou,[20] A. N. Zhu,[64] J. Zhu,[43] K. Zhu,[1] K. J. Zhu,[1,58,64] K. S. Zhu,[12,g] L. Zhu,[34] L. X. Zhu,[64] S. H. Zhu,[71] T. J. Zhu,[12,g] W. D. Zhu,[41] Y. C. Zhu,[72,58] Z. A. Zhu,[1,64] J. H. Zou,[1] and J. Zu,[72,58]

(BESIII Collaboration)

[1]*Institute of High Energy Physics, Beijing 100049, People's Republic of China*
[2]*Beihang University, Beijing 100191, People's Republic of China*
[3]*Bochum Ruhr-University, D-44780 Bochum, Germany*
[4]*Budker Institute of Nuclear Physics SB RAS (BINP), Novosibirsk 630090, Russia*
[5]*Carnegie Mellon University, Pittsburgh, Pennsylvania 15213, USA*
[6]*Central China Normal University, Wuhan 430079, People's Republic of China*
[7]*Central South University, Changsha 410083, People's Republic of China*
[8]*China Center of Advanced Science and Technology, Beijing 100190, People's Republic of China*
[9]*China University of Geosciences, Wuhan 430074, People's Republic of China*
[10]*Chung-Ang University, Seoul, 06974, Republic of Korea*

[11]COMSATS University Islamabad, Lahore Campus, Defence Road,
Off Raiwind Road, 54000 Lahore, Pakistan

[12]Fudan University, Shanghai 200433, People's Republic of China

[13]GSI Helmholtzcentre for Heavy Ion Research GmbH, D-64291 Darmstadt, Germany

[14]Guangxi Normal University, Guilin 541004, People's Republic of China

[15]Guangxi University, Nanning 530004, People's Republic of China

[16]Hangzhou Normal University, Hangzhou 310036, People's Republic of China

[17]Hebei University, Baoding 071002, People's Republic of China

[18]Helmholtz Institute Mainz, Staudinger Weg 18, D-55099 Mainz, Germany

[19]Henan Normal University, Xinxiang 453007, People's Republic of China

[20]Henan University, Kaifeng 475004, People's Republic of China

[21]Henan University of Science and Technology, Luoyang 471003, People's Republic of China

[22]Henan University of Technology, Zhengzhou 450001, People's Republic of China

[23]Huangshan College, Huangshan 245000, People's Republic of China

[24]Hunan Normal University, Changsha 410081, People's Republic of China

[25]Hunan University, Changsha 410082, People's Republic of China

[26]Indian Institute of Technology Madras, Chennai 600036, India

[27]Indiana University, Bloomington, Indiana 47405, USA

[28a]INFN Laboratori Nazionali di Frascati, I-00044, Frascati, Italy

[28b]INFN Sezione di Perugia, I-06100, Perugia, Italy

[28c]University of Perugia, I-06100, Perugia, Italy

[29a]INFN Sezione di Ferrara, I-44122, Ferrara, Italy

[29b]University of Ferrara, I-44122, Ferrara, Italy

[30]Inner Mongolia University, Hohhot 010021, People's Republic of China

[31]Institute of Modern Physics, Lanzhou 730000, People's Republic of China

[32]Institute of Physics and Technology, Peace Avenue 54B, Ulaanbaatar 13330, Mongolia

[33]Instituto de Alta Investigación, Universidad de Tarapacá, Casilla 7D, Arica 1000000, Chile

[34]Jilin University, Changchun 130012, People's Republic of China

[35]Johannes Gutenberg University of Mainz, Johann-Joachim-Becher-Weg 45, D-55099 Mainz, Germany

[36]Joint Institute for Nuclear Research, 141980 Dubna, Moscow region, Russia

[37]Justus-Liebig-Universitaet Giessen, II. Physikalisches Institut, Heinrich-Buff-Ring 16,
D-35392 Giessen, Germany

[38]Lanzhou University, Lanzhou 730000, People's Republic of China

[39]Liaoning Normal University, Dalian 116029, People's Republic of China

[40]Liaoning University, Shenyang 110036, People's Republic of China

[41]Nanjing Normal University, Nanjing 210023, People's Republic of China

[42]Nanjing University, Nanjing 210093, People's Republic of China

[43]Nankai University, Tianjin 300071, People's Republic of China

[44]National Centre for Nuclear Research, Warsaw 02-093, Poland

[45]North China Electric Power University, Beijing 102206, People's Republic of China

[46]Peking University, Beijing 100871, People's Republic of China

[47]Qufu Normal University, Qufu 273165, People's Republic of China

[48]Renmin University of China, Beijing 100872, People's Republic of China

[49]Shandong Normal University, Jinan 250014, People's Republic of China

[50]Shandong University, Jinan 250100, People's Republic of China

[51]Shanghai Jiao Tong University, Shanghai 200240, People's Republic of China

[52]Shanxi Normal University, Linfen 041004, People's Republic of China

[53]Shanxi University, Taiyuan 030006, People's Republic of China

[54]Sichuan University, Chengdu 610064, People's Republic of China

[55]Soochow University, Suzhou 215006, People's Republic of China

[56]South China Normal University, Guangzhou 510006, People's Republic of China

[57]Southeast University, Nanjing 211100, People's Republic of China

[58]State Key Laboratory of Particle Detection and Electronics, Beijing 100049,
Hefei 230026, People's Republic of China

[59]Sun Yat-Sen University, Guangzhou 510275, People's Republic of China

[60]Suranaree University of Technology, University Avenue 111, Nakhon Ratchasima 30000, Thailand

[61]Tsinghua University, Beijing 100084, People's Republic of China

[62a]Turkish Accelerator Center Particle Factory Group, Istinye University, 34010, Istanbul, Turkey

[62b]Near East University, Nicosia, North Cyprus, 99138, Mersin 10, Turkey

[63a]University of Bristol, H H Wills Physics Laboratory

[63b]*University of Bristol, Tyndall Avenue*
[63c]*University of Bristol, Bristol*
[63d]*University of Bristol, BS8 1TL*
[64]*University of Chinese Academy of Sciences, Beijing 100049, People's Republic of China*
[65]*University of Groningen, NL-9747 AA Groningen, The Netherlands*
[66]*University of Hawaii, Honolulu, Hawaii 96822, USA*
[67]*University of Jinan, Jinan 250022, People's Republic of China*
[68]*University of Manchester, Oxford Road, Manchester, M13 9PL, United Kingdom*
[69]*University of Muenster, Wilhelm-Klemm-Strasse 9, 48149 Muenster, Germany*
[70]*University of Oxford, Keble Road, Oxford OX13RH, United Kingdom*
[71]*University of Science and Technology Liaoning, Anshan 114051, People's Republic of China*
[72]*University of Science and Technology of China, Hefei 230026, People's Republic of China*
[73]*University of South China, Hengyang 421001, People's Republic of China*
[74]*University of the Punjab, Lahore-54590, Pakistan*
[75a]*University of Turin and INFN, University of Turin, I-10125, Turin, Italy*
[75b]*University of Eastern Piedmont, I-15121, Alessandria, Italy*
[75c]*INFN, I-10125, Turin, Italy*
[76]*Uppsala University, Box 516, SE-75120 Uppsala, Sweden*
[77]*Wuhan University, Wuhan 430072, People's Republic of China*
[78]*Yantai University, Yantai 264005, People's Republic of China*
[79]*Yunnan University, Kunming 650500, People's Republic of China*
[80]*Zhejiang University, Hangzhou 310027, People's Republic of China*
[81]*Zhengzhou University, Zhengzhou 450001, People's Republic of China*

[a]Deceased.

[b]Also at the Moscow Institute of Physics and Technology, Moscow 141700, Russia.

[c]Also at the Novosibirsk State University, Novosibirsk, 630090, Russia.

[d]Also at the NRC "Kurchatov Institute", PNPI, 188300, Gatchina, Russia.

[e]Also at Goethe University Frankfurt, 60323 Frankfurt am Main, Germany.

[f]Also at Key Laboratory for Particle Physics, Astrophysics and Cosmology, Ministry of Education; Shanghai Key Laboratory for Particle Physics and Cosmology; Institute of Nuclear and Particle Physics, Shanghai 200240, People's Republic of China.

[g]Also at Key Laboratory of Nuclear Physics and Ion-beam Application (MOE) and Institute of Modern Physics, Fudan University, Shanghai 200443, People's Republic of China.

[h]Also at State Key Laboratory of Nuclear Physics and Technology, Peking University, Beijing 100871, People's Republic of China.

[i]Also at School of Physics and Electronics, Hunan University, Changsha 410082, China.

[j]Also at Guangdong Provincial Key Laboratory of Nuclear Science, Institute of Quantum Matter, South China Normal University, Guangzhou 510006, China.

[k]Also at MOE Frontiers Science Center for Rare Isotopes, Lanzhou University, Lanzhou 730000, People's Republic of China.

[l]Also at Lanzhou Center for Theoretical Physics, Lanzhou University, Lanzhou 730000, People's Republic of China.

[m]Also at the Department of Mathematical Sciences, IBA, Karachi 75270, Pakistan.

[n]Also at Ecole Polytechnique Federale de Lausanne (EPFL), CH-1015 Lausanne, Switzerland.

[o]Also at Helmholtz Institute Mainz, Staudinger Weg 18, D-55099 Mainz, Germany.

[p]Also at School of Physics, Beihang University, Beijing 100191, China.